

Artemis 3 Lunar Environment Monitoring Station (LEMS-A3) Thermal Control Subsystem Architecture

Ethan Burbridge[1]
Vertex Aerospace, LLC, Grasonville, Maryland, 21368

Juan Rodriguez-Ruiz[2]
NASA Goddard Space Flight Center, 8800 Greenbelt Rd., Greenbelt, MD 20771

The NASA Artemis 3 Lunar Environment Monitoring Station (LEMS-A3) instrument will be deployed by the Artemis 3 crew in the South Pole region of the Moon. LEMS-A3 consists of a common services bus and two seismometers to be buried in the regolith, and the instrument has been repackaged to improve the performance of the bus Thermal Control Subsystem (TCS). The nighttime heat leak has been reduced from 3.98 W to 1.528 W, from Engineering Design Unit (EDU) Thermal Vacuum (TVAC) to the as predicted for the LEMS-A3 Critical Design Review (CDR). This improvement was brought about by repackaging that reduces surface area for the Integrated Multi-Layer Insulation (IMLI), optimizing harness passthroughs including the selection of cryogenic coaxial cables, selecting an improved differential thermal expansion heat switch, and redesign of the Launch Lock (LL). The upgraded configuration enables LEMS-A3 to continuously operate in and survive the lunar night for a design life of 24 lunations (approx. two Earth years) to meet extended-operation mission objectives. This paper discusses the repackaging, thermal design improvements, and upgraded thermal hardware.

Acronyms and Nomenclature

a	=	Moon Ecliptic Aberration
ALSEP	=	Apollo Lunar Surface Experiment Package
BB	=	BroadBand sonde/seismometer
CBE	=	Current Best Estimate
CDR	=	Critical Design Review
C&DH	=	Command and Data Handling
EDU	=	Engineering Design Unit
EPS	=	Electrical Power System
DSN	=	Deep Space Network
FPGA	=	Flight Programmable Gate Array
GSFC	=	Goddard Space Flight Center
HLS	=	Human Landing System
HMS	=	Hibernation Management System
LEMS-A3	=	Lunar Environment Monitoring Station – Artemis 3
JPL	=	Jet Propulsion Laboratory
LGA	=	Low Gain Antenna
LVPC	=	Low Voltage Power Card
IMLI	=	Integrated Multi-Layer Insulation
MEV	=	Maximum Expected Value
MGA	=	Medium Gain Antenna
MLI	=	Multi-Layer Insulation
NASA	=	National Aeronautics and Space Administration
SC	=	Spacecraft
SP	=	Short Period sonde/seismometer
TCS	=	Thermal Control Subsystem

[1] Thermal Engineer, 8800 Greenbelt Rd, Greenbelt, MD 20771
[2] Thermal Principal Design Lead, 8800 Greenbelt Rd, Greenbelt, MD 20771

TRL = Technology Readiness Level
β_{SC} = Spacecraft Beta Angle
ϕ = Deployment Latitude
$\theta_{surface}$ = Local Surface Inclination Relative to Horizon
θ_{SC} = Spacecraft Inclination Relative to Horizon

I. Introduction

LEMS-A3 is an autonomous remote seismic monitoring station to be deployed to the South Pole region of the Moon via the Artemis 3 crew. The seismic suite consists of two three-axis sondes that will be buried in the lunar regolith to detect seismic events which consist of shallow moonquakes, deep moonquakes, meteoroid impacts, and thermal cycling. For science objectives focused on the South Pole region, LEMS-A3 will be gathering the first seismic data for the region which will inform objectives and requirements for future missions in that region. The LEMS-A3 seismic suite will expand upon data gathered by the Apollo Lunar Surface Experiment Package (ALSEP) and other planned lunar surface instruments.

LEMS-A3 includes all systems necessary for remote operation like direct-to-earth communications, solar power generation, battery storage, command and data handling, and thermal control. Figure 1 details the system architecture. Novel to this system is a low-power Hibernation Mode which disables all systems like communications and data processing not related to science gathering or system telemetry. LEMS-A3 will operate in this Hibernation Mode 98.6% of the mission to conserve power. The Hibernation Mode is controlled via the Hibernation Management System (HMS) which nominally operates continuously over the two-year mission. Once every 24 hours, for 20 minutes, HMS will enable the Command and Data Handling card (C&DH) which maintains the operations schedule based on timekeeping in the HMS. During this 20 minute "Awake" period, the C&DH will determine the charge state of the battery and the solar power incident on the solar arrays based on the two sun sensors and enable or disable the Electrical Power System (EPS) as appropriate. Figure 2 pictures the concept of operations which includes at least one monthly, three-hour, direct-to-Earth communications window using the Deep Space Network (DSN) for downloading science data and system telemetry. Additional short-duration, 20-minute, communication windows can be performed using smaller antenna dishes for monitoring system health and uploading mission schedules.

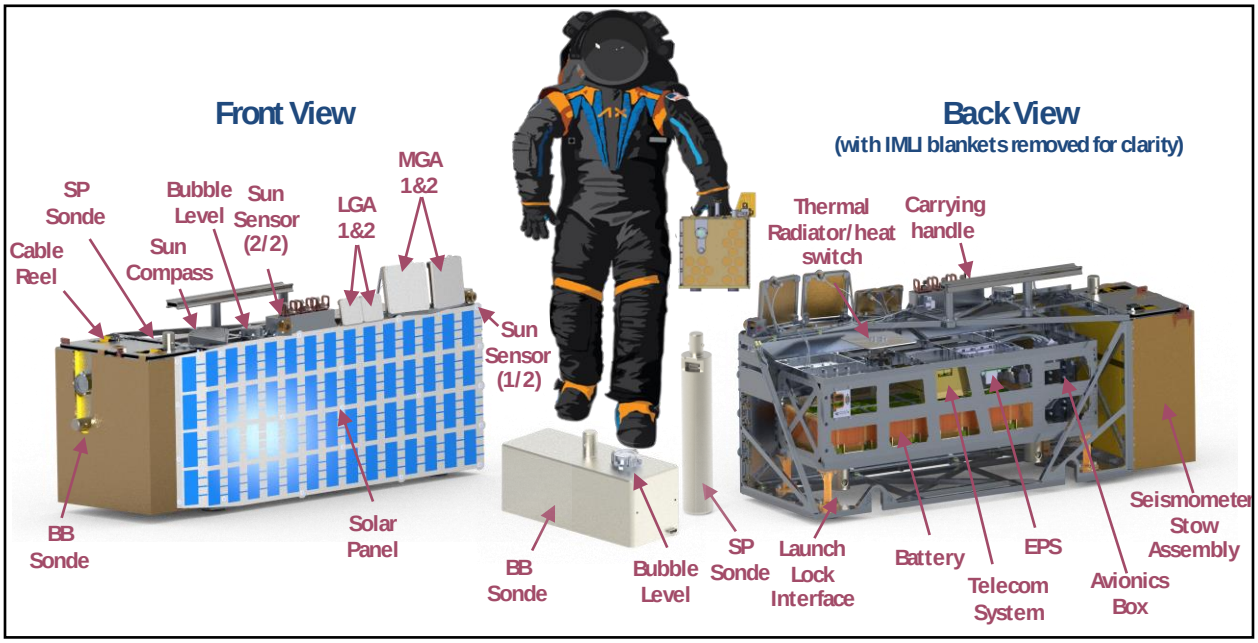

Figure 1. LEMS-A3 components.

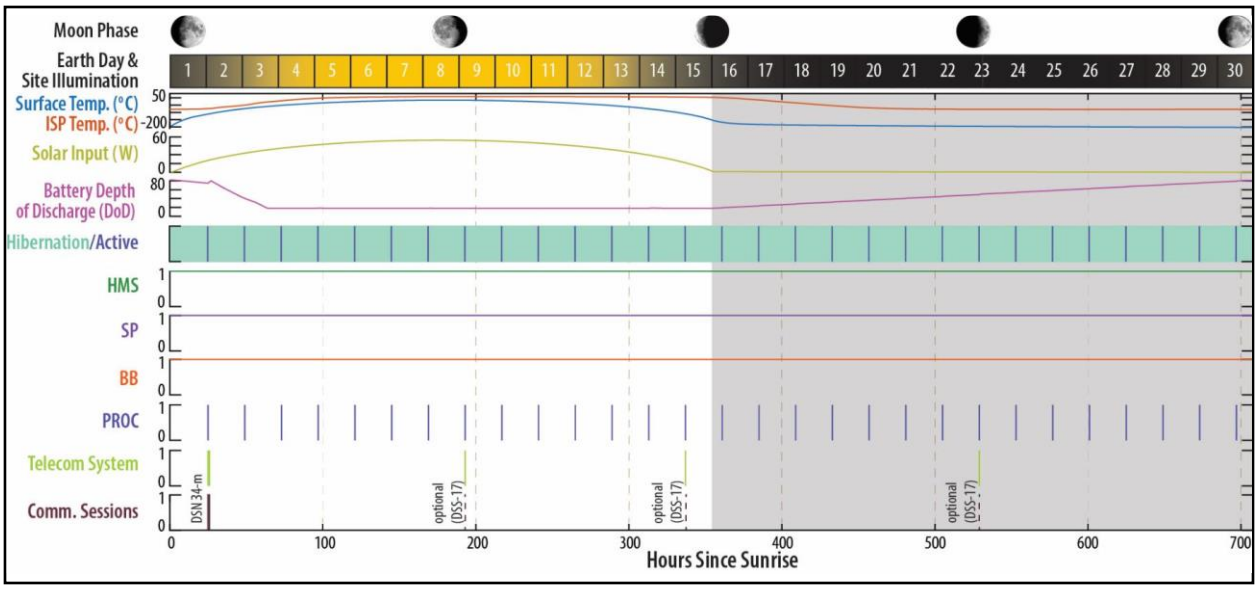

Figure 2. LEMS-A3 Concept of Operations.

From 2018 to 2022, the LEMS prototype was developed and tested under the NASA Development of Advanced Lunar Instruments program to elevate the design to a NASA Technology Readiness Level (TRL) of 6. The TVAC testing conducted as a part of the TRL-6 effort validated the design to operate in the minimum and maximum predicted temperatures with margin. In this test, the nighttime thermal energy leak was measured to be 1407.3 Wh for 354 hours or the equivalent of a continuous power of 3.98 W[3].

At CDR, the LEMS-A3 was required to demonstrate the feasibility of the Thermal Control Subsystem (TCS) in the representative worst case cold and hot environments expected on the lunar surface. To demonstrate mission success, the TCS must maintain the LEMS-A3 bus within temperature limits during all operational and non-operational modes. Furthermore, the total nighttime energy used for temperature maintenance must be shown to be less than 640 Wh of allocated battery energy for a 354 hr period between sun illuminations.

II. Thermal Architecture

The design presented is the flight TCS design as it stands at the CDR. Figure 3 details the TCS architecture and the relationship between the various components. All temperature sensitive components like the avionics, battery, EPS, and radio are isolated from the environment inside the LEMS-A3 bus. The bus thermal interfaces are carefully controlled at the four primary heat leak paths: the launch lock, signal and power passthrough (SAPP) harnessing, Integrated Multi-Layer Insulation (IMLI), and heat switch as shown in Figure 4. Components that are required to interact with the environment like the solar array, antennae, and astronaut interfaces are mounted to the superstructure via an uncontrolled thermal interface. The temperatures of the external components are managed with thermal control coatings but are expected to experience temperatures ranging from -200°C to +115°C.

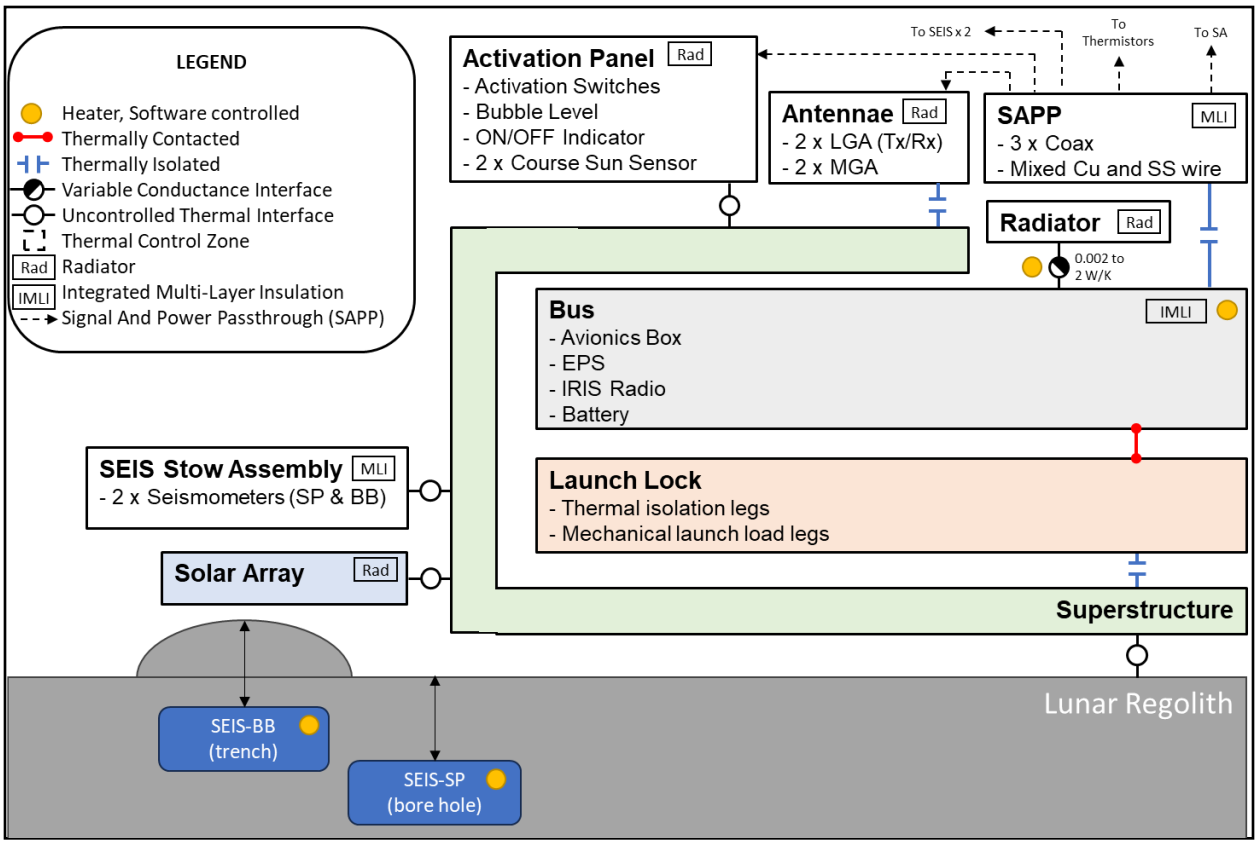

Figure 3. Bus TCS block diagram.

Bus and seismometer temperatures are maintained with four software-controlled Kapton foil heaters. The circuits are controlled by the HMS using a deadband control algorithm with active temperature monitoring. One heater is mounted to the bus and is nominally set to -28/-26°C. The heat switch has a heater mounted to its housing and is discussed more in Section II.D: Heat Switch and Radiator. The other two heater services are supplied to the seismometers for their TCS.

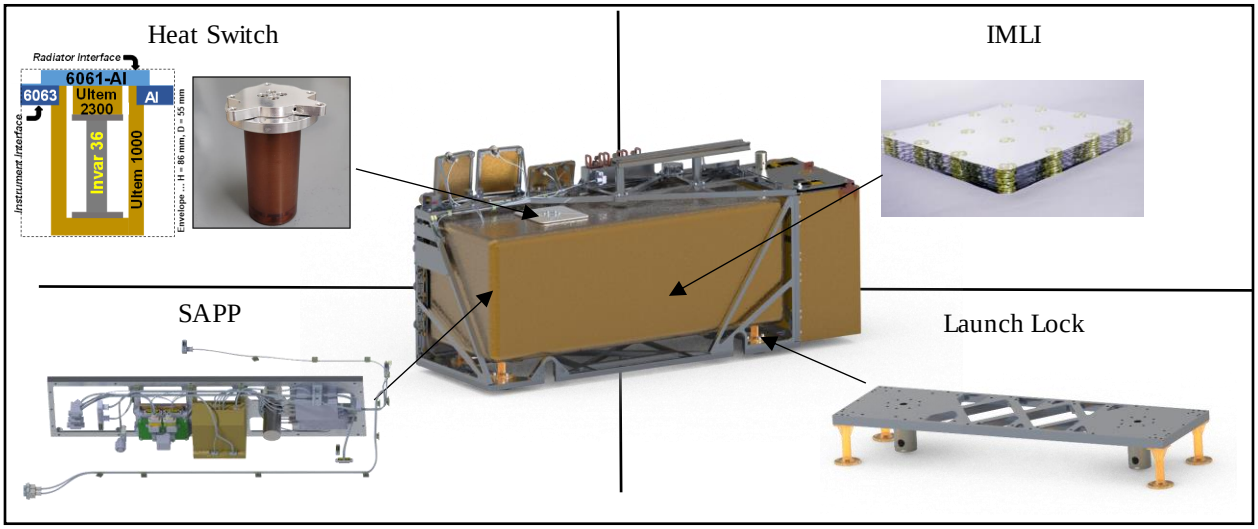

Figure 4. Bus heat leak paths.

A. Launch Lock

The launch lock shown in Figure 5 is an astronaut-actuated interface designed to handle launch loads aboard the SpaceX Starship Human Landing System (HLS) while meeting thermal conductance isolation requirements when deployed on the lunar surface. Two nested titanium mechanical legs are constrained by pins during launch to handle most of the launch loads. After arrival on the lunar surface, an astronaut removes the pins and carries the LEMS-A3 instrument package to the deployment site. Once deployed on the lunar surface, the only contact between the internal structure of the bus and the external environment is through the four ULTEM 1000 standoffs.

In addition to meeting launch and thermal requirements, the launch lock separates the thermal and mechanical design of externally mounted components, namely the solar array, CSS, antennae, and astronaut interfaces. Without the launch lock and the superstructure, external components would need to be mounted to the bus structure via standoffs which would increase the system heat leak and increase design time since mechanical and thermal engineers would have to iterate many more designs.

To mitigate risk of dust accumulation or regolith contact, the titanium mechanical posts and ULTEM thermal legs are coated with a low emissivity coating. The thermal legs will be shrouded with a Kapton™ film cylinder to act as a radiation and sun shield. Relative to the total heat leak, the thermal conductivity of the mechanical legs is high enough that they are effectively the same temperature as the bus internal components. Since the mechanical legs stick out past the thermal blanketing, there is a risk that the legs will contact the lunar regolith should deployment create a mound underneath the LEMS bus. To mitigate this risk, the solar array dust cover is wrapped underneath the launch lock to increase the bearing surface area and decrease subsidence into the regolith.

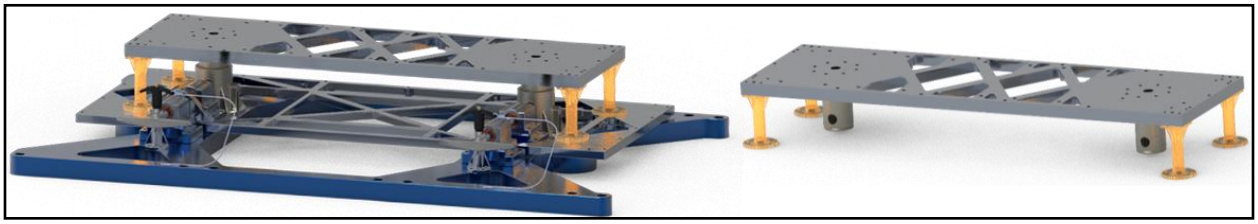

Figure 5. (left) Launch lock stowed. (right) Launch lock deployed.

B. Integrated Multi-Layer Insulation

The LEMS-A3 bus radiation heat loss is minimized using an 18-layer IMLI consisting of double aluminized Kapton film with an outer layer of laminated Nextel™ fabric and Stamet™. IMLI differs from standard MLI blankets in that the layers are separated with a proprietary low thermal conductivity tripod spacer technology rather than plastic mesh fabric. The layup can be seen in Figure 6.

This technology improves blanket performance for small systems in three ways. First, the discrete spacers reduce layer-to-layer conduction losses by a factor of 1000 compared to mesh fabric. Second, the separation of the layers allows edges to be closed out layer by layer so that edge losses are minimized. Finally, the spacers can be metallized with vapor deposited aluminum that is a few hundred Angstroms thick to ground the blanketing with no additional conducted heat loss. The net effect is an effective emissivity less than 0.0028 as measured during the TRL-6 development testing[2].

The outer layer includes a layer of Nextel™ ballistic shielding to protect the LEMS bus from hyper-velocity regolith particles generated during HLS liftoff. The LEMS-A3 team partnered with the NASA Engineering and Safety Center to analyze the impact of the liftoff plume on the LEMS bus and to select the ballistic shielding to prevent penetration of the LEMS-A3 bus IMLI thus ensuring blanket thermal performance and protecting internal components.

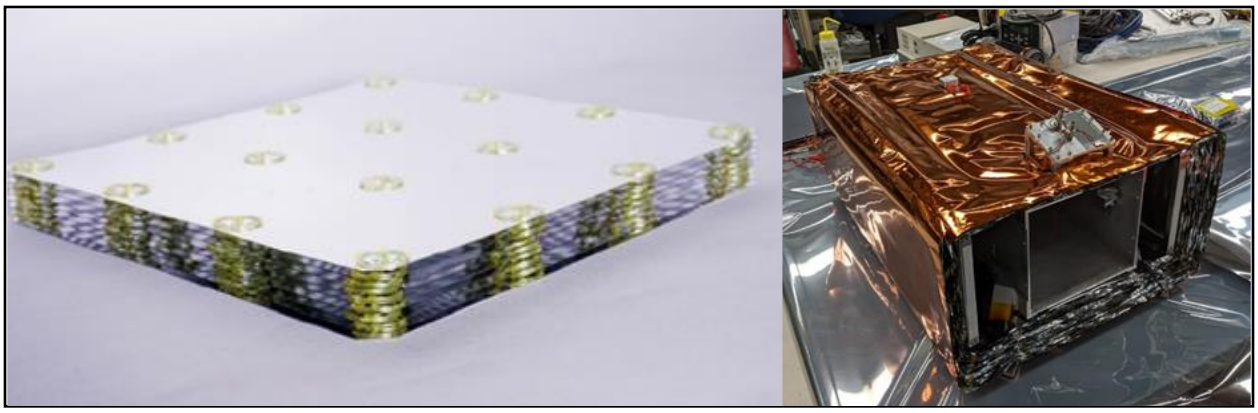

Figure 6. (left) IMLI Sample. (right) TRL-6 Test Article showing IMLI cross section.

C. Signal and Power Passthrough Harnessing

Harnessing passing through the IMLI including wires for seismometer power and signal, solar array power, antennae coax, and temperature sensors was optimized to minimize thermal conductance while meeting power and signal quality requirements. All low power harnessing was manganin for the stretch going from inside the IMLI to outside. Harnessing carrying higher levels of current like the solar array power lines and the seismometer power lines is copper. The SAPP harnessing is isolated from the internal bus structure and the superstructure on ULTEM Clickbond™ standoffs to minimize heat loss through the SAPP. Figure 7 details the harnessing routing path.

The antenna radio frequency signals are carried on semi-rigid, cupronickel coaxial cables adapted from the cryogenics industry. The coaxial cables were optimized by selecting diameters and materials that met the 2 dB maximum attenuation requirement but minimized the thermal conductance. Several dozen part numbers were compared for each of the four antennas to minimize the thermal conductance for a given run length. The result was a 57% reduction in the expected heat leak during nighttime for the coaxial cables compared to copper coaxial cables.

All SAPP harnessing will be blanketed to minimize heat loss from radiation. The SAPP harnessing in the cold operational steady state case bridges the internal thermal zone at -30°C to the external thermal zones at approximately -200°C making radiation heat loss significant if not mitigated. SAPP harnessing inside the IMLI will be wrapped with 6-layer MLI with aluminized Kapton outer layer. SAPP harnessing external to the IMLI will have the same stackup with the external layer swapped for Stamet. Harnessing that will be exposed to the HLS launch plume will have an additional layer of Nextel™ fabric for ballistic shielding.

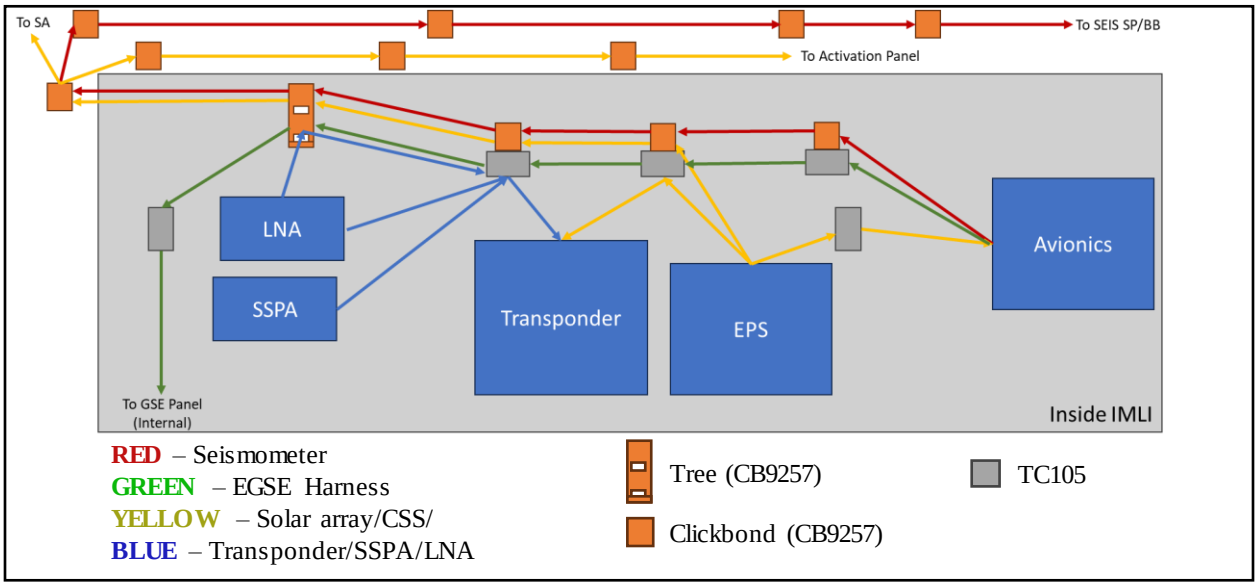

Figure 7. SAPP block diagram.

D. Heat Switch and Radiator

The heat switch is a reverse differential coefficient of thermal expansion device that connects or disconnects two aluminum plates. Above the switching temperature at 0°C, the plates are pressed together and heat flows at approximately 5 W/°C. Below the switching temperature, the plates are separated, and the primary heat flow path is through the ULTEM housing to the INVAR 36 internal rod. This torturous path has a conductance below 0.002 W/°C[1].

A heater is mounted to the ULTEM 1000 housing to allow active control of the heat switch actuation. Without the heater, the bus temperature rises to +30°C before the heat switch closes. This effect is caused by the radiator lowering the average temperature of the heat switch when the aluminum plates are not in contact. The result is that the bus temperature can be well above the heat switch switching temperature without the plates contacting. With the heater, the heat switch can be enabled at dawn when the bus temperature is much colder so that the LEMS-A3 bus has more thermal energy storage capacity before the radio temperature limits are reached.

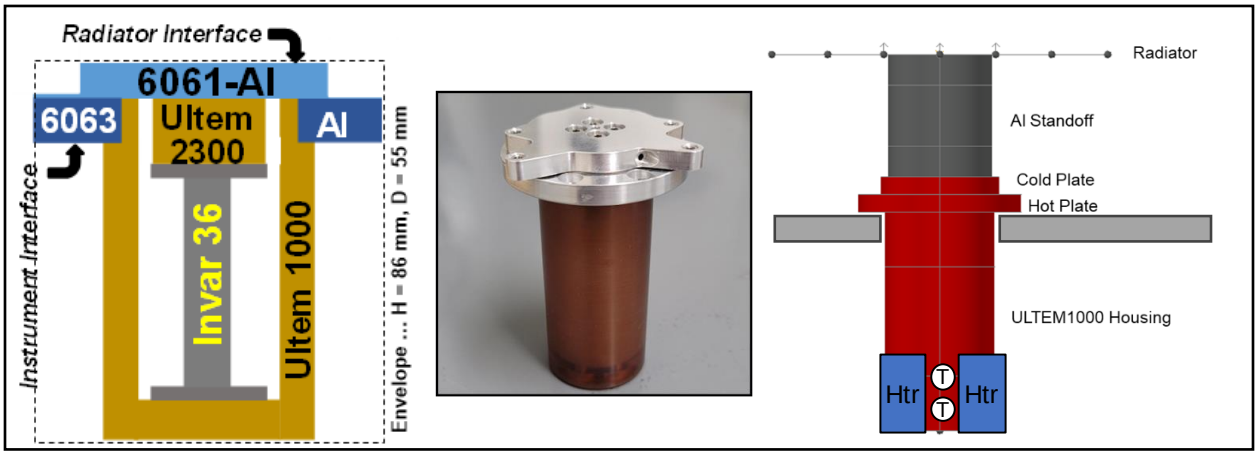

Figure 8. (left) heat switch cross section. (center) photo of assembled heat switch. Courtesy Dave Bugby and JPL. (right) thermal model of heat switch and radiator assembly.

E. Solar Array Radiator

Power generation is achieved with a flexible solar array mounted to the sun-facing side of the LEMS-A3 superstructure. The solar array was selected to avoid cover glass which is an astronaut safety hazard and to reduce mass. Given the solar array is body-mounted, additional area was added to the sun-facing side to radiate heat and cool the array to improve power generation efficiency. The cells as seen in Figure 9 are spaced out so that each cell has a border radiator equal in size to that cell. Since the array is solar cells sandwiched between polyimide sheets, a graphite sheet is laminated to the back of the solar array to spread heat from the solar cells to the cell radiators.

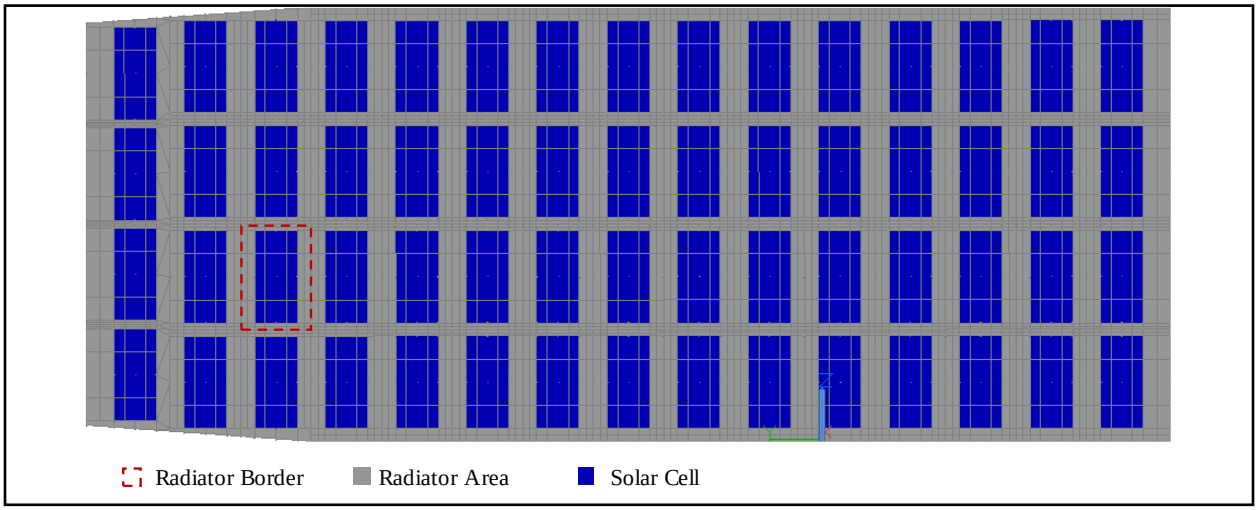

Figure 9. Solar Array Thermal Design

III. Thermal Analysis Assumptions

The thermal analysis was completed in the geometric and math model developed in ANSYS Thermal Desktop seen in Figure 10. It includes all flight hardware in the surface deployed configuration except for the seismometer sondes which are deployed in the subsurface in an independent thermal model. The seismometer sondes and the bus are sufficiently thermally isolated such that independent modeling is adequate.

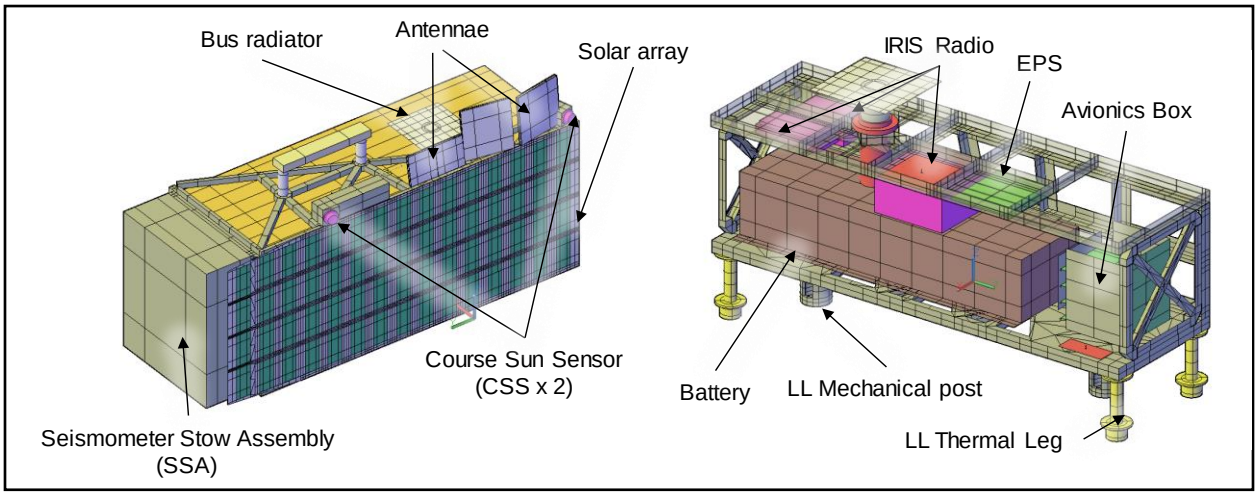

Figure 10. Thermal Desktop model.

The LEMS-A3 system is being developed in parallel with the Artemis mission architecture and Concept of Operations so some details, specifically site selection, and their associated requirements have yet to be defined. The proposed landing regions encompass approximately 8000 km^2 of varying terrain (Figure 11). The specifics of the deployment site like latitude, elevation, surface inclination, near-field terrain, and far-field terrain are design drivers for the LEMS-A3 TCS. To encompass the possible worst case cold and hot thermal environments, a survey of the proposed landing regions was conducted using the LRO Lunar QuickMap. The survey was constrained by site requirements for the HLS since the landing vehicle will take preference over the instrument. These analysis assumptions are condensed into Table 1.

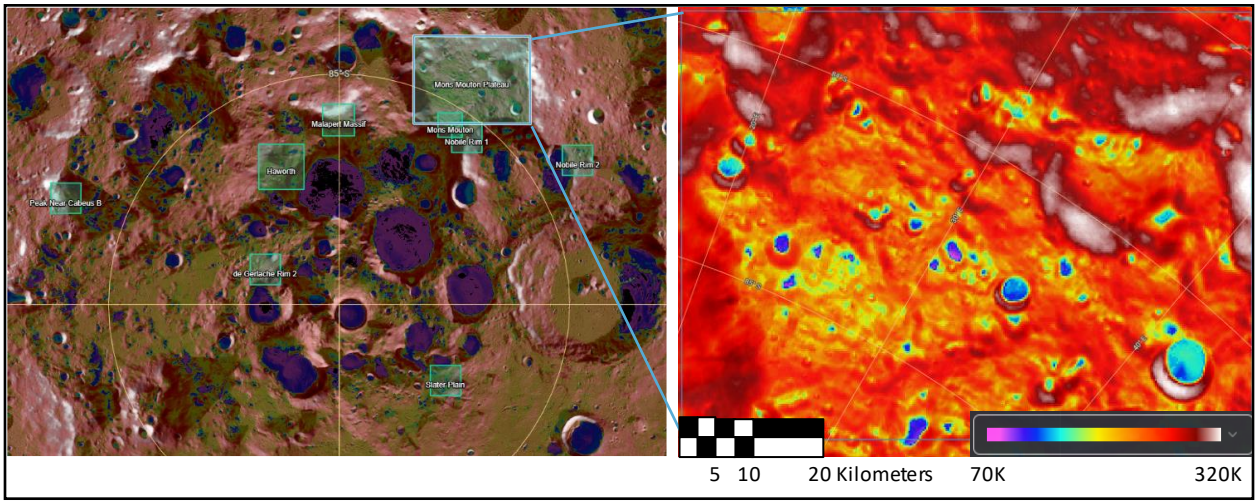

Figure 11. (left) Artemis 3 candidate landing regions. (right) Mons Mouton Plateau summer max temperature map. (LRO Lunar QuickMap)

Table 1. Thermal analysis assumptions.

Case Name		Steady State Cold Op	Steady State Hot Op	Transient Cold Op	Transient Hot Op
Power State	Op Mode	3	3	See Figure 12	See Figure 12
	Biasing	CBE	MEV		
Coatings BOL/EOL Biasing		BOL	EOL + dust	BOL	EOL + dust
Environment	Local Lunar Time	5:30	12:00	One Lunation	One Lunation
	Solar Heat Flux	1310	1426	1310	1426
	Lunar IR Emissivity	0.95	0.98	0.95	0.98
	Lunar Albedo	N/A	0.47	0.53	0.47
Spacecraft Attitude	Latitude	90	83.5	90	83.5
	Moon Aberration	0	1.543	0	1.543
	Surface Inclination	0.0	10.0	0.0	10.0
	Spacecraft Inclination	0.0	-5.0	-5.0	-5.0
	Effective Spacecraft Beta Angle	0	13.053	0	13.053
Bus Radiator Terrain Derate[1]		100%	85%	100%	85%

Table 2. Bus power modes.

		Hibernation		**Monthly 3-hr Comms**		**Battery Charging (Daytime)**		**Op Daily Data Download**	
State Number (For Figure 12)		**3**		**6**		**10**		**12 (CBE) 11 (MEV)**	
Duration [min]		**Continuous**		**180**		**Continuous**		**10 min daily**	
Tabulation		**CBE**	**MEV**	**CBE**	**MEV**	**CBE**	**MEV**	**CBE**	**MEV**
Avionics	CDH	OFF	OFF	1.900	1.995	OFF	OFF	1.900	1.995
	HMS	0.419	0.548	0.419	0.548	0.419	0.548	0.419	0.548
	HMSD	0.201	0.361	0.201	0.361	0.201	0.361	0.201	0.361
	LVPC	0.230	0.306	0.705	0.805	0.230	0.306	0.705	0.805
	SSC	0.140	0.147	0.140	0.147	0.140	0.147	0.140	0.147
Power	EPS	0.168	0.176	1.400	1.470	1.400	1.470	1.400	1.470
	Battery	0.073	0.077	1.903	1.998	0.135	0.141	0.253	0.266
Comms	SSPA	OFF	OFF	12.700	13.335	OFF	OFF	OFF	OFF
	LNA	OFF	OFF	0.507	0.532	OFF	OFF	OFF	OFF
	Transponder	OFF	OFF	15.993	16.793	OFF	OFF	OFF	OFF
Instrument	SEIS1	0.150	0.158	0.150	0.158	0.150	0.158	0.150	0.158
	SEIS2	0.150	0.158	0.150	0.158	0.150	0.158	0.150	0.158
Internal Heat Subtotal		**1.23**	**1.62**	**35.87**	**37.99**	**2.53**	**2.98**	**5.02**	**5.60**
External Heat Subtotal		**0.30**	**0.32**	**0.30**	**0.32**	**0.30**	**0.32**	**0.30**	**0.32**
RF Transmitted		**0.00**	**0.00**	**3.80**	**3.80**	**0.00**	**0.00**	**0.00**	**0.00**
Total Power		**1.53**	**1.94**	**39.97**	**42.33**	**2.83**	**3.31**	**5.32**	**5.92**

The LEMS-A3 bus includes representative heat loads on all relevant components with Current Best Estimate (CBE) values used for cold operational analysis and Maximum Expected Value (MEV) used for hot operational analysis (Table 2). Between the cold and hot analysis the bus heat dissipation varies from 1.23 W to 3.31 W which is a driver for the design of the thermal isolation systems and the need for the heat switch. During daily data downloads the power is expected to spike as high as 5.92 W. The monthly three-hour communication transient with an MEV heat dissipation inside the LEMS-A3 bus of 37.99 W is the driver for the hot case. Figure 12 shows how the bus heat dissipation is varied during transient analysis for a lunation.

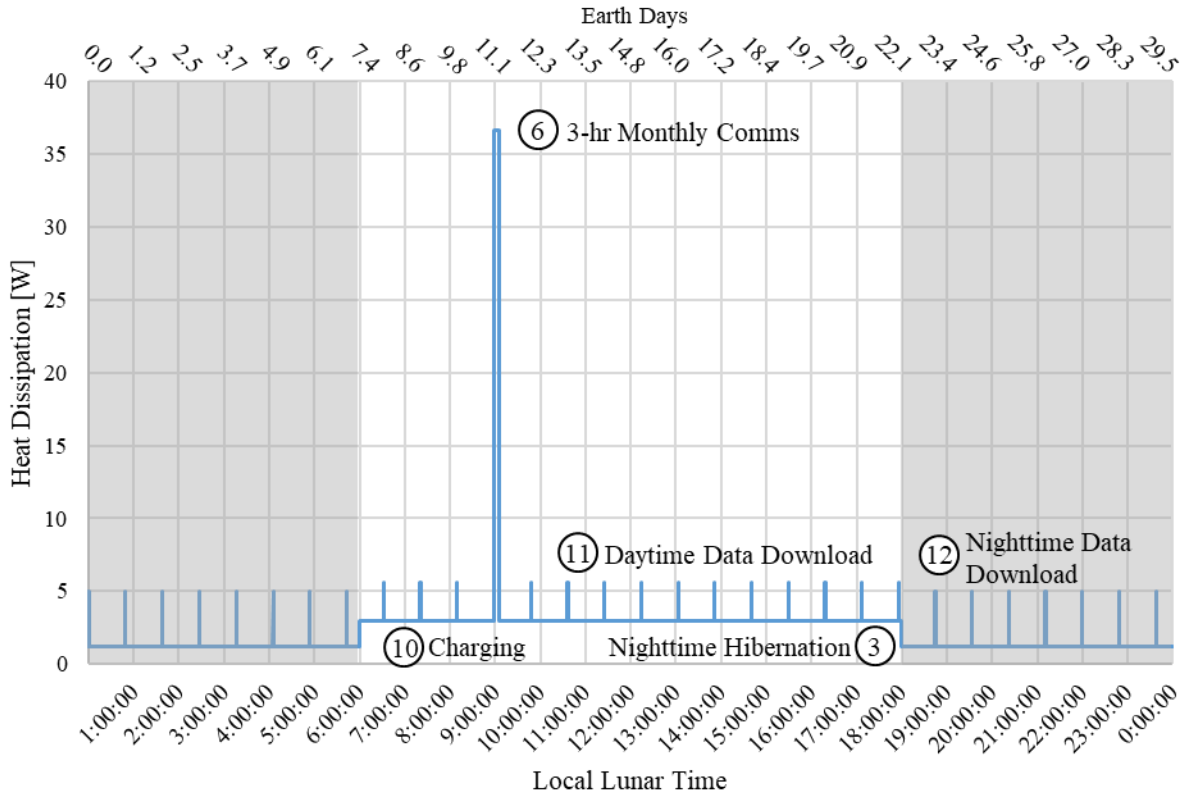

Figure 12. Lunation transient heat load profile.

The properties of the lunar surface thermal environment are defined by the *Cross-Program Design Specification for Natural Environments Revision G*[8] and *Human Landing System Lunar Thermal Analysis Guidebook*[6]. The environment properties are varied to create the worst case cold and hot environments relative to the operation of the LEMS-A3. The temperature of the lunar surface is dominated by interactions with the sun rather than subsurface heat flows so priority was given to matching surface temperatures over subsurface temperatures.

Eq. 1 details the calculation for the effective spacecraft beta angle (β_{SC}), where ϕ is the deployment latitude, a is the moons aberration, $\theta_{surface}$ is the local surface inclination relative to the horizon, and θ_{SC} is the spacecraft inclination relative to the horizon. $\theta_{surface} + \theta_{SC}$ will always be less than 5° because astronauts will level the LEMS-A3 bus using a bubble level.

$$\beta_{SC} = (90° - \phi) + a + \theta_{surface} + \theta_{SC} \quad (1)$$

The thermal analysis is further biased by varying surface optical properties and thermophysical properties to their minimum and maximum values for a two-year mission. Thermophysical properties are taken from temperature-dependent curves for common cryogenic materials provided by the National Institute for Standards and Technology[5]. The optical properties are provided by the Goddard Space Flight Center Coatings Branch based on heritage performance and expected conditions in the South Pole region. These are detailed in Table 3.

Lunar dust is an uncertain input to the performance of thermal control coatings. To address lunar dust, LEMS-A3 has implemented hardware solutions like dust covers for deployment and assumed a worst-case End-of-Life dust accumulation for evaluating the impact on thermal control coatings. The dust covers protect critical surfaces like the solar array and radiator during deployment in the event the astronauts drop LEMS-A3 in the regolith. Dust cover removal is one of the last steps in the system deployment to minimize dust kicked up by astronauts from settling on surfaces. To address dust accumulation during the 2-yr mission, LEMS-A3 adopted the assumptions developed by the VIPER mission which is 10% accumulation per year. Some of the dust is expected to fall on other dust particles so at end-of-life, an accumulation of 19% is expected. To determine the effect on coatings, the worst-case optical properties of dust particles is averaged with the coating property at End-of-Life. In cases where the dust accumulation would result in cooler optical properties compared to no dust accumulation, the former is assumed. This is only seen for infrared emissivity where the darker dust will cause the value to increase; therefore, only the solar absorptivity (α) is considered in Eq. 2. A value of 0.57 is assumed for dust solar absorptance as a worst-case assumption.

$$\alpha' = \alpha_{EOL}(0.81) + (0.57)(0.19) \tag{2}$$

Table 3. Thermal optical coatings properties with End-of-Life, and lunar dust deratings.

Coating	BOL			EOL			EOL α Dust Obscuration (α = 0.53)			
	α	ε	α/ε	α	ε	α/ε	% Area	α	ε	α/ε
5 mil Silver Teflon	0.08	0.79	0.10	0.2	0.75	0.27	19%	0.27	0.75	0.35
5 mil Aluminum Tape	0.18	0.09	2.00	0.22	0.02	11.00	No Change			
Aluminum Anodize, Black	0.73	0.84	0.87	0.88	0.78	1.13	No Change			
Aluminum Anodize, Clear	0.30	0.84	0.36	0.4	0.78	0.51	19%	0.43	0.78	0.55
Aluminum, Polished	0.12	0.05	2.40	0.16	0.03	5.33	No Change			
Aluminum, Iridite	0.32	0.18	1.78	0.5	0.04	12.50	No Change			
Tiodize™, Black	0.82	0.50	1.64	0.82	0.50	1.64	No Change			
Invar 36	1.00	0.30	3.33	1.00	0.30	3.33	No Change			
5 mil Kapton	0.51	0.74	0.69	0.51	0.74	0.69	No Change			
Solar Array, Cells	0.683	0.85	0.80	0.90	0.79	1.14	19%	0.83	0.79	1.05
Solar Array, Radiator	0.16	0.85	0.19	0.22	0.75	0.29	19%	0.28	0.75	0.38
Aluminized Kapton	0.07	0.05	1.40	0.11	0.02	5.50	19%	0.19	0.02	9.70
Goldized Kapton	0.21	0.07	3.00	0.25	0.03	8.33	19%	0.31	0.07	4.37
Z93 White Coating	0.14	0.93	0.15	0.14	0.93	0.15	No Change			
Z93C55 White Coating	0.11	0.94	0.12	0.30	0.88	0.34	19%	0.35	0.88	0.39
ULTEM 2300	1.00	0.50	2.00	1.00	0.50	2.00	No Change			

IV. Thermal Analysis Results

The LEMS-A3 project follows the *GSFC-STD-7000b*[4] and the *GSFC-STD-1000H*[5] standards for applying temperature margin to components. Table 4 and Table 5 show margin meeting this standard of greater than 5°C in green. Predicts with less than 5°C of margin are shown in yellow except for components under active heater control which require no margin on the minimum predict relative to limits. The one component with negative margin, the solar array, is shown in red. It is expected that the operational limit of the solar array will be increased for qualification testing to accommodate the prediction. The transient results have a slightly more benign thermal environment due to thermal inertia of the LEMS-A3 bus and the lunar regolith. On the hot side the transient thermal analysis includes the monthly, 3-hr communication session which results in higher maximum temperatures compared to steady state.

The steady-state predictions shown in Table 4 are considered conservative relative to the transient predictions shown in Table 5 because the steady-state predictions do not consider thermal mass. For this reason, the heater prediction from the cold op steady-state analysis are used for accounting the system heat leaks. However, the hot op steady-state case does not account for varying power modes like the 3-hr monthly comms, so the hot op transient case is used for validating maximum temperatures are within limits.

Table 4. Steady state thermal analysis predictions.

Description	Active Heater Control	Op Limits [°C]		Cold Op Steady State		Hot Op Steady State	
				Predict	Margin	Predict	Margin
		Min	Max	[°C]	Min	[°C]	Max
Avionics, PROC	x	-35	60	-24.8	10.2	35.2	24.8
Avionics, HMS	x	-35	60	-24	11	36.3	23.7
Avionics, HMS-D	x	-35	60	-24.4	10.6	35.9	24.1
Avionics, LVPC	x	-35	60	-24.6	10.4	35.4	24.6
Avionics, Special Services	x	-35	60	-24.4	10.6	35.6	24.4
Battery	x	-35	50	-27.2	7.8	31.4	18.6
LGA RX		-210	70	-189.9	20.1	34	36
LGA TX		-210	70	-190.1	19.9	36.9	33.1
IRIS LNA	x	-30	60	-27.6	2.4	29	31
MGA 1		-210	70	-189.5	20.5	17.9	52.1
MGA 2		-210	70	-189.4	20.6	17	53
IRIS SSPA	x	-30	60	-27.5	2.5	29	31
IRIS Transponder	x	-30	60	-27.3	2.7	30.4	29.6
EPS	x	-30	60	-27	3.0	32.5	27.5
CSS 1		-200	80	-189.2	10.8	31.9	48.1
CSS 2		-200	80	-190.7	9.3	47.6	32.4
Bus Radiator		No Limit		-115.9	-	13.1	-
Bus Heat Switch		-200	50	-27.7	-172.3	27.2	23.8
Solar Array		-200	110	-199.5	0.5	115.6	-5.6
Regolith Surface, Sun side		No Limit		-198.5	-	105.6	-
Regolith Surface, Natural		No Limit		-202.7	-	28.9	-

Figure 13 shows the transient plot of the hot op transient statistics seen in Table 5. The changing power modes of the LEMS-A3 bus can be seen in the temperature spikes on the plot. The small spikes of approximately 5°C in the avionics box are the daily data downloads (Power Modes 11/12). The large transient spike a few days into daytime is the monthly 3-hr communications session (Power Mode 6) which results in a large temperature spike. Also notice the points at which the heat switch heater controller enables or disables. There is a delay between the heater switching state and the heat switch opening or closing due to thermal inertia of the system.

Table 5. Transient thermal analysis predictions.

Description	Active Heater Control	Op Limits [°C]		Cold Op Transient Predict [°C]		Cold Op Transient Margin	Hot Op Transient Predict [°C]		Hot Op Transient Margin
		Min	Max	Min	Max	Min	Min	Max	Max
Avionics, PROC	x	-35	60	-26.0	23.1	9.0	-23.8	44.4	15.6
Avionics, HMS	x	-35	60	-25.2	20.7	9.8	-23.2	42.2	17.8
Avionics, HMS-D	x	-35	60	-25.6	20.4	9.4	-23.5	41.8	18.2
Avionics, LVPC	x	-35	60	-25.8	21.3	9.2	-23.7	42.6	17.4
Avionics, Special Services	x	-35	60	-25.6	20.1	9.4	-23.4	41.5	18.5
Battery	x	-35	50	-28.8	12.5	6.2	-26.3	34.7	15.3
LGA RX		-210	70	-188.9	-107.9	21.1	-188.8	19	51.0
LGA TX		-210	70	-189.0	-99.8	21.0	-189	21.2	48.8
IRIS LNA	x	-30	60	-29.4	29.3	0.6	-27.2	51.5	8.5
MGA 1		-210	70	-188.5	-124.9	21.5	-188.5	3.6	66.4
MGA 2		-210	70	-188.4	-130.8	21.6	-188.3	4.3	65.7
IRIS SSPA	x	-30	60	-29.2	35.3	0.8	-27	57.4	2.6
IRIS Transponder	x	-30	60	-28.8	32.4	1.2	-26.5	54.3	5.7
EPS	x	-30	60	-28.5	29.0	1.5	-26.2	50.8	9.2
CSS 1		-200	80	-188.1	-128.8	11.9	-188.1	22.7	57.3
CSS 2		-200	80	-189.6	-77.7	10.4	-189.5	29.6	50.4
Bus Radiator		No Limit		-129.4	3.2	-	-119.8	28.7	-
Bus Heat Switch		-200	50	-29.2	26.0	170.8	-27	48.3	2.7
Solar Array		-200	110	-198.6	-163.2	1.4	-199	107.2	2.8
Regolith Surface, Sun side		No Limit		-197.9	-194.2	-	-197.6	79.2	-
Regolith Surface, Natural		No Limit		-204.6	-204.5	-	-202.7	-57.8	-

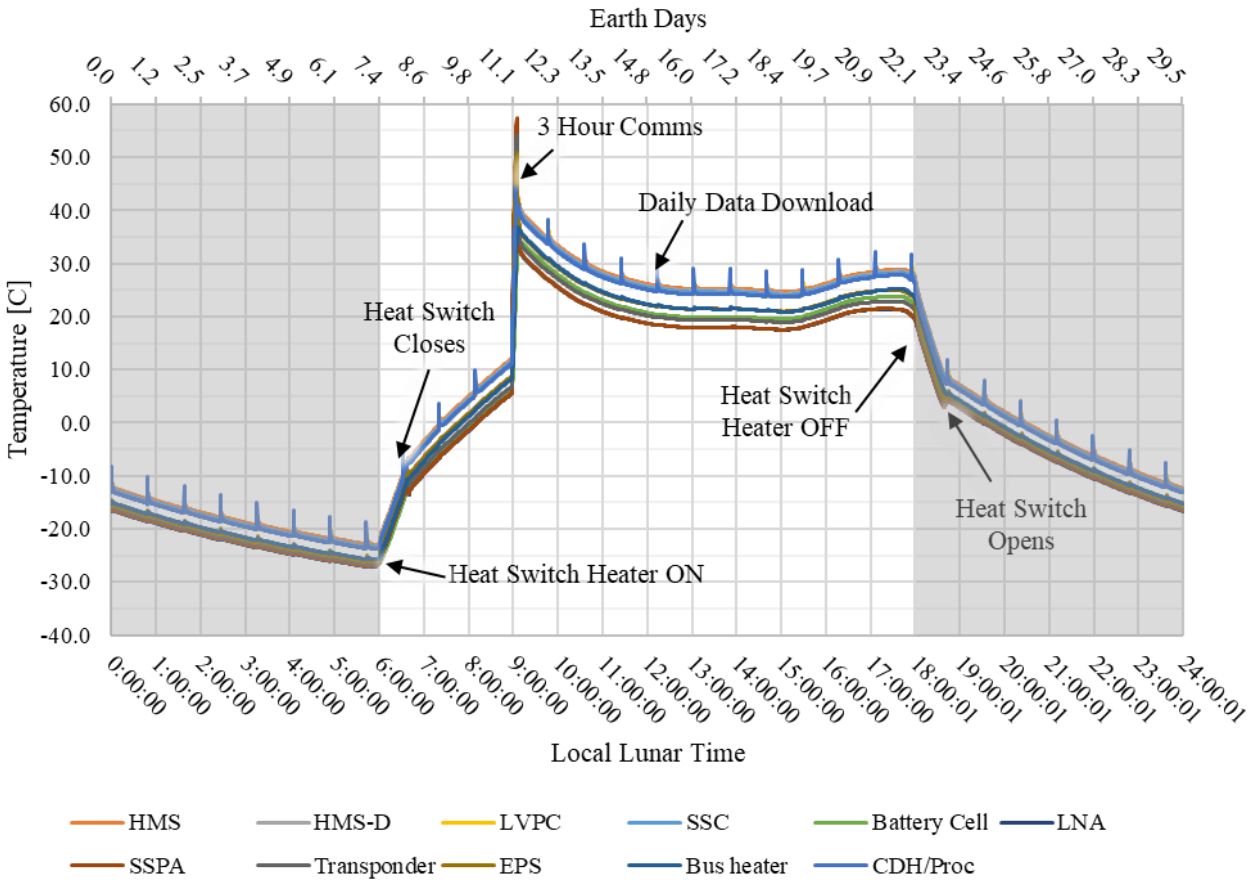

Figure 13. Transient Hot Operational Transient Results for Internal Components

The cold operational steady state heat flow results presented in Figure 14 show that the LEMS-A3 bus meets its battery energy allocation with 15% margin. This table does not include energy stored in thermal mass which is estimated to be 3.7 Wh/°C. The thermal mass is not considered since the temperature change between nighttime and daytime operation can be as little as 10°C. If needed, the on-board, software-controlled heaters can be used to preheat the bus prior to night.

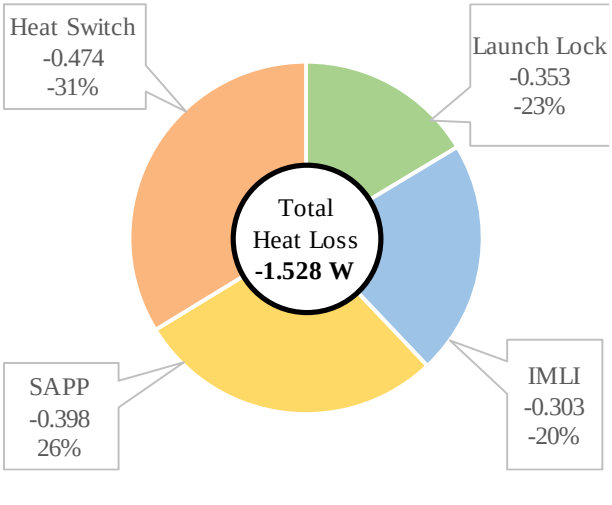

Description	Heat Balance [W]
Launch Lock	-0.353
IMLI	-0.303
Signal and Power Passthrough	-0.398
Heat Switch	-0.474
Total Heat Loss	-1.528
Internal Electronics CBE Heat	1.231
Heater Power	0.297
Total Bus Internal Electronics Power	1.528
Thermal Energy Balance (354 hr) [Wh]	541
Allocated Battery Energy [Wh]	640
Battery Thermal Energy Margin [Wh]	99 (15%)
Time to Exceedance [days]	17.7

Figure 14. LEMS-A3 Bus Heat Loss during Cold Operational Steady State

V. Conclusion

The LEMS-A3 bus thermal architecture has been developed for flight to the level of maturity appropriate for a critical design review. Temperature, heat leak, and heater predictions have been generated assuming worst case cold and hot parameters in a representative environment on the lunar surface. An exceedance in the solar arrays has been identified and a path forward for resolution has been developed to reduce the maximum expected temperature.

The LEMS-A3 bus thermal architecture has been improved since the TRL-6 development effort. The nighttime heat leak as analyzed at missions CDR was determined to be 1.528 W for 354 hr or 541 Wh. Compared to the TRL-6 effort which measured the heat leak at 3.98 W, the TCS heat leak was reduced 2.452 W or 61%. The CDR heat leak shows 15% margin. Should this margin hold, the additional capacity would allow the LEMS-A3 bus TCS to stay within its battery energy allocation for 425 hours, an additional 65 hours beyond the mission life.

Acknowledgments

The efforts of the LEMS engineering and science teams are acknowledged for their tireless work in bringing this mission design to fruition in such a short time. This quality of science instrumentation has been made possible by the collaboration of the team members and their attention to detail.

Lunar QuickMap (https://lunar.quickmap.io), a collaboration between NASA, Arizona State University & Applied Coherent Technology Corp, is acknowledged for the use of its imagery.

References

[1]Birmingham, W., Schunk, G., & Evans, B. (2024). Lunar Latitude And Terrain Radiator Sensitivity Study. *Thermal and Fluids Analysis Workshop*. Cleveland. Retrieved from https://tfaws.nasa.gov/wp-content/uploads/TFAWS2024-PT-25-Paper.pdf

[2]Bugby, D., & Rivera, J. (2020). High Performance Thermal Switch for Lunar and Planetary Surface Extreme Environments. Online: Texas Tech University Libraries. Retrieved from https://hdl.handle.net/2346/86389

[3]Burbridge, E., Benna, M., & Hamann, M. (2023). Lunar Environment Monitoring Station TRL-6 Thermal. *International Conference on Environmental Systems.* Calgary, CA: Texas Tech University Libraries. Retrieved from https://hdl.handle.net/2346/94722

[4](2023). *GSFC-STD-1000H, Goddard Space Flight Center Rules for the Design, Development, Verification, and Operation of Flight.* National Aeronautics and Space Administration, Goddard Space Flight Center. NASA Technical Standards System.

[5](2021). *GSFC-STD-7000b, General Environmental Verification Standard (GEVS) for GSFC Flight Programs and Projects.* National Aeronautics and Space Administration, Goddard Space Flight Center. NASA Technical Standards System.

[6]Hamill, B. D., Schunk, R. G., & Erickson, L. R. (2021). *Human Landing System Lunar Thermal Analysis Guidebook.* National Aeronautics and Space Administration. NASA Technical Reports Server.

[7]P.E., B., R., R., & M.A., L. (2006). Cryogenic Material Properties Database. *ICMC '06 Twenty First International Cryogenic Engineering Conference and 9th Cryogenics* (pp. 13-21). Prague, CZ: Icaris Ltd.

[8]Roberts, B. (2019). *Cross-Program Design Specification for Natural Environments, Rev. G.* National Aeronautics and Space Administration, Marshall Space Flight Center. Alabama, United States: NASA Technical Reports Server.